Quadratic integration over the three-dimensional Brillouin zone

1991 J. Phys.: Condens. Matter 3 6721

(http://iopscience.iop.org/0953-8984/3/35/005)

J. Phys.: Condens. Matter 3 (1991) 6721–6742. Printed in the UK

Quadratic integration over the three-dimensional Brillouin zone

G Wiesenekker and E J Baerends
Department of Theoretical Chemistry, Free University, De Boelelaan, 1081 HV Amsterdam, The Netherlands

Received 24 September 1990

Abstract. A new method is described to evaluate integrals of quadratically interpolated functions over the three-dimensional Brillouin zone. The method is based on the method of the authors for analytic quadratic integration over the two-dimensional Brillouin zone. It uses quadratic interpolation not only for the dispersion relation $\varepsilon(\boldsymbol{k})$, but for property functions $f(\boldsymbol{k})$ as well. The method allows a 'machine accuracy' evaluation of the integrals and may therefore be regarded as equivalent to a truly analytic evaluation of the integrals. It is compared to other methods of integral approximation by calculating tight-binding Brillouin zone integrals using the same number of k-points for all methods. Also shown are cohesive energy calculations for a number of elements. When the quadratic method is compared to the commonly used linear method, it is found that far fewer k-points are needed to obtain a desired accuracy.

1. Introduction

Calculation of properties of solids with m-dimensional translation symmetry ($m = 1, 2, 3$) requires the evaluation of integrals such as [1]

$$J(E) = \sum_n \int_V f_n(\boldsymbol{k})\theta(E - \varepsilon_n(\boldsymbol{k}))\,\mathrm{d}^m k \tag{1}$$

or its derivative

$$I(E) = \frac{\mathrm{d}J(E)}{\mathrm{d}E} = \sum_n \int_V f_n(\boldsymbol{k})\delta(E - \varepsilon_n(\boldsymbol{k}))\,\mathrm{d}^m k = \sum_n \int_{E=\varepsilon_n(\boldsymbol{k})} \frac{f_n(\boldsymbol{k})}{|\nabla\varepsilon_n(\boldsymbol{k})|}\,\mathrm{d}S \tag{2}$$

where E is the energy for which the property has to be calculated, the summation is over the energy bands, V is the volume of the first Brillouin zone, $f_n(\boldsymbol{k})$ is a property function for the nth band, θ and δ are the step and delta function respectively, and $\varepsilon_n(\boldsymbol{k})$ is the dispersion relation for the nth band. If, for example, $f_n(\boldsymbol{k}) \equiv 1$, $I(E)$ is the density of states for energy E: DOS(E). As can be seen from (1) and (2), $J(E)$ is an integral over the volume lying 'below' the surface $E = \varepsilon_n(\boldsymbol{k})$, whereas $I(E)$ is an integral over the surface $E = \varepsilon_n(\boldsymbol{k})$. Energies for which $|\nabla\varepsilon_n(\boldsymbol{k})| = 0$ on the surface $E = \varepsilon_n(\boldsymbol{k})$ are known as Van Hove singularities. Generally, $I(E)$ or $\mathrm{d}I(E)/\mathrm{d}E$ is infinite at Van Hove energies [2, 3]. Usually the analytical form of the functions $f_n(\boldsymbol{k})$ or $\varepsilon_n(\boldsymbol{k})$ is not known, so the integrals $J(E)$ and $I(E)$ have to be evaluated by numerical integration. As bandstructure calculations are time consuming and the time needed for such calculations usually increases

0953-8984/91/356721 + 22 $03.50

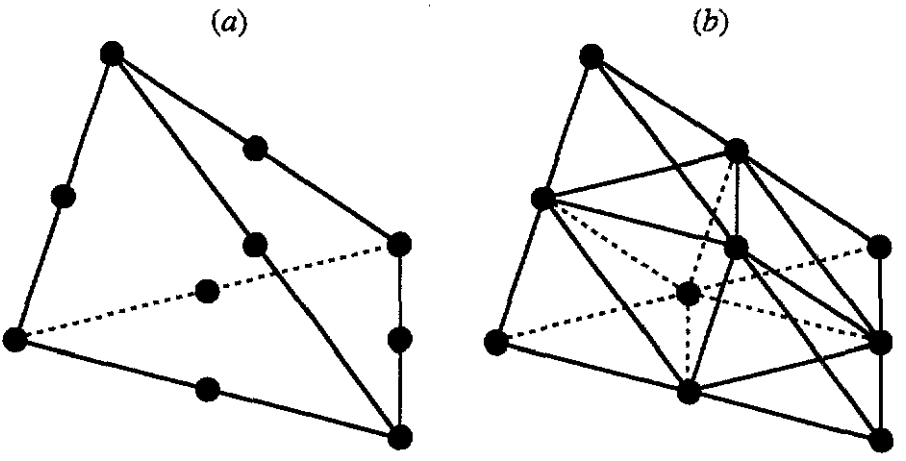

Figure 1. (*a*) Linear interpolation uses the values of the functions $f(k)$ and $\varepsilon(k)$ in the k-points at the corners of the primary tetrahedron. Quadratic interpolation uses the values of the functions $f(k)$ and $\varepsilon(k)$ in the k-points at the corners and the edges of the tetrahedron. (*b*) In comparisons (see section 4) the same number of k-points should be used, so the primary tetrahedron used in the quadratic interpolation is divided into eight smaller tetrahedra with k-points at the corners in which linear interpolation can be used.

linearly with the number of k-points used, the question rises how the integrals $I(E)$ and $J(E)$ can be accurately evaluated using as few k-points as possible.

The method commonly used for the numerical evaluation of the integrals is the following: the first Brillouin zone can always be partitioned into a number of so-called basic or primary simplices (triangles in two dimensions, tetrahedra in three dimensions). The evaluation of the integrals $I(E)$ and $J(E)$ in one simplex is considered. If the k-points for which the band structure calculation is performed are at the corners of the simplex, it is possible to obtain a linear approximation to the dispersion relation $\varepsilon(k)$ and the function $f(k)$ using the known values at the corners. With these linear functions it is possible to evaluate $I(E)$ and $J(E)$ analytically [4–10]. The linear approximation on which this so-called linear tetrahedron method (LTM) is based, may be expected to be more accurate when the size of the simplices decreases, i.e. the mesh of k-points becomes finer. However, if E is at or close to a Van Hove singularity, it is well known that the linear approximation breaks down and a quadratic approximation is essential [11, 12]. A quadratic approximation is obtained in the basic simplex if also the values of $f(k)$ and $\varepsilon(k)$ are available at k-points on the midpoints of the edges (see figure 1). Unfortunately, it is not a simple matter to evaluate the integrals analytically if $f(k)$ and $\varepsilon(k)$ in (1) and (2) are substituted with quadratic polynomials. An overview of the methods found in the literature is given in table 1, from which it appears that a fully quadratic method with exact evaluation (i.e. to machine accuracy, either analytically or numerically) of the integrals is not yet available for three-dimensional systems. We will argue below that such a scheme is indeed highly desirable and will present an exact fully quadratic method for three-dimensional systems in this paper.

For three-dimensional systems the two most important quadratic approaches to date are the hydrid tetrahedron method (HTM) of MacDonald *et al* [16] and the projective-geometry method (PGM) of Methfessel *et al* [17–19]. In the PGM the integrals are evaluated exactly, using geometric methods, but only for a linear interpolation of $f(k)$. We have shown in the two-dimensional case [20], that significant improvement is obtained for

Table 1. An overview of the methods found in the literature for the evaluation of the integrals $I(E)$ and $J(E)$. Shown is the order of interpolation of the functions $\varepsilon(k)$ and $f(k)$, the type of integral evaluation of $I(E)$ and $J(E)$ and the dimension m for which the method has been implemented. The entries analytic and numerical stand for potentially exact evaluations in the sense that machine accuracy can be obtained by judicious avoidance of build up and round-off errors (analytic) or use of sufficient points in a standard (e.g. Gauss–Legendre) one-dimensional numerical integration (numerical). The qualification 'approximate' for the hybrid tetrahedron method is discussed in the text.

$f(k)$	$\varepsilon(k)$	$I(E)$	$J(E)$	Abbreviation	m	
constant	linear	analytic	analytic		1, 2, 3	[14]
linear	linear	analytic	analytic	LTM	1, 2, 3	[4–10]
linear	quadratic	analytic	numerical	PGM	1, 2, 3	[17–19]
quadratic	quadratic	approximate	approximate	HTM	1, 2, 3	[15, 16]
quadratic	quadratic	analytic	numerical	AQM	1, 2	[20]

quadratic interpolation of $f(k)$ (the analytic quadratic method (AQM)). Understandably, this improvement is particularly striking when $f(k)$ exhibits considerable variation over the Brillouin zone. In this paper we will show that the same holds true for the three-dimensional case (see figure 10 and compare to figure 7 of [20]).

The HTM is very attractive for its simplicity. Within a given primary tetrahedron the quadratic approximations $f_q(k)$ and $\varepsilon_q(k)$ to $f(k)$ and $\varepsilon(k)$ are obtained. The integrals $I(E)$ and $J(E)$ over the primary tetrahedron are then evaluated by subdividing the primary tetrahedron into smaller ones and using the LTM in these secondary tetrahedra. At the corners of the secondary tetrahedra the values of $f_q(k)$ and $\varepsilon_q(k)$ are used, so no additional bandstructure calculations are needed. The HTM is in fact an approximate numerical evaluation of the integrals $I(E)$ and $J(E)$, with $f_q(k)$ and $\varepsilon_q(k)$ substituted for $f(k)$ and $\varepsilon(k)$, over the primary tetrahedron. MacDonald *et al* used a subdivision of the primary tetrahedron into 64 secondary ones, but this number may of course be increased to achieve convergence of the 'inner' numerical integration. We would like to point out, however, that the HTM, although a distinct improvement on the LTM, runs into the same kind of problem at Van Hove energies as the LTM itself. The linear approximation in the secondary tetrahedrons partly cancels the effect of the quadratic approximation in the primary tetrahedron. This may be seen as follows. The essential shortcoming of the linear approximation is its inability to describe a possible extremum of $\varepsilon(k)$ somewhere in a tetrahedron. A quadratic approximation $\varepsilon_q(k)$ to $\varepsilon(k)$ may however exhibit extrema, and use of $\varepsilon_q(k)$ in an exact evaluation of e.g. the integral $I(E)$ (2) will then account for the important effect of the occurring zeros $|\nabla\varepsilon_n(k)| = 0$ of the denominator. If however the integral is evaluated by using the LTM in small secondary tetrahedrons, the extremum of $\varepsilon_q(k)$ will be missed again. The advantage of the HTM is of course that the number of secondary tetrahedrons can be made large with little extra cost, but since nothing has been done about the essential deficiency of the linear method one still expects the convergence of the 'inner' numerical integration to obtain $I(E)$ and $J(E)$ to be poor. To illustrate these remarks a few examples may be in order.

In figure 2 we give an example of the convergence of the density of states DOS(E) in the HTM with the number of secondary tetrahedra in the 'normal' situation, that is, not close to a Van Hove singularity. The primary tetrahedron here has corners (0, 0, 0), (1, 0, 0), (0, 1, 0), and (0, 0, 1) and the dispersion relation is taken perfectly spherical, $\varepsilon(k) = x^2 + y^2 + z^2$ (x stands for k_x, etc), and $E = 0.5$, so we are integrating over the surface $x^2 + y^2 + z^2 = 0.5$, which has considerable but by no means unrealistic curvature

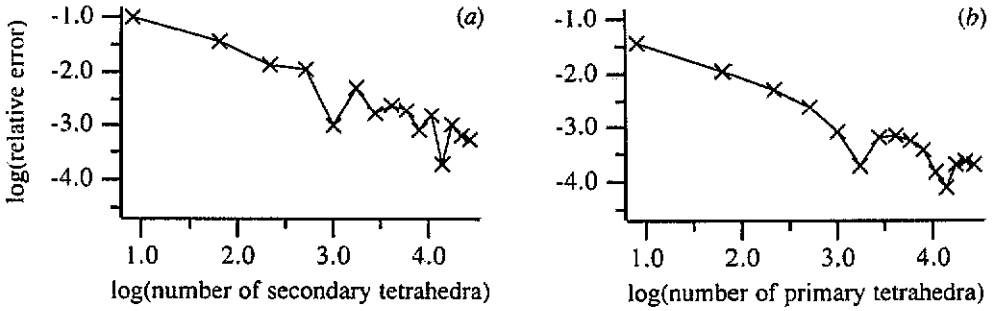

Figure 2. (*a*) Percentage error in the density of states as a function of the number of secondary tetrahedra in the HTM if the quadratic surface is the sphere $x^2 + y^2 + z^2 = 0.5$ and the primary tetrahedron is (0, 0, 0), (1, 0, 0), (0, 1, 0), (0, 0, 1). (*b*) Convergence of the density of states in the 'standard' HTM method with the number of primary tetrahedra if the quadratic surface is $x^2 + y^2 + z^2 = 0.5$ and the IBZ is the tetrahedron (0, 0, 0), (1, 0, 0), (0, 1, 0), (0, 0, 1). A primary tetrahedron is now always divided into 64 smaller tetrahedra.

over the primary tetrahedron. The energy is far from the Van Hove singularity at $E = 0$. This example of course also demonstrates the performance of just the LTM.

As can be seen from figure 2(*a*) a reasonable (~0.1%) accuracy may be obtained but convergence is fairly slow and at least a division of the primary tetrahedron in 1024 smaller tetrahedra is required to obtain an accuracy of (only) 1%. It is possible to improve the accuracy at a given number of subdivisions (but not the convergence rate), obtaining an average accuracy of e.g. ~1% at 64 smaller tetrahedrons as in the work of MacDonald *et al* [16] and Reser [13], by choosing smaller primary tetrahedrons so that the constant-energy surface is effectively flatter. This is illustrated by the example in figure 2(*b*) of the performance of the 'standard' HTM where a constant subdivision into 64 tetrahedra for the 'inner' integration is used and only the number of primary tetrahedrons is varied. (Here the tetrahedron with corners (0, 0, 0), (1, 0, 0), (0, 1, 0), and (0, 0, 1) may be looked upon as the IBZ that is being subdivided into primary tetrahedrons). We note that a genuine quadratic method, such as Methfessel *et al* [17–19] and the one we propose in this paper, would have zero error in this example of a perfectly quadratic dispersion relation.

However, the hybrid method can fail particularly badly in the neighbourhood of Van Hove singularities. The quadratic surface $E = x^2 + y^2 + z^2$ has a Van Hove singularity for $E = 0$. In figure 3(*a*) the convergence of the HTM with the number of secondary tetrahedra is given for an energy very near this Van Hove singularity ($E = 0.005$). The convergence is very slow indeed, the error being practically 100% up to quite large numbers of secondary tetrahedra. The reason is that the part of the surface $x^2 + y^2 + z^2 = 0.005$ lying within the primary tetrahedron is very small, and many divisions into smaller tetrahedra are needed before the spherical surface is represented with any accuracy by flat triangles in a number of small tetrahedra. The standard HTM (figure 3(*b*)) does not do much better. A genuine quadratic method still gives zero error.

As another example figure 4 gives the convergence of the standard HTM and our quadratic method with the number of primary tetrahedra if the dispersion relation is not perfectly quadratic, but of the simple-cubic tight-binding type: $\epsilon(x, y, z) = -(\cos(\pi x) + \cos(\pi y) + \cos(\pi z))/3$. There are Van Hove singularities for $E = -1$ and $E = -1/3$ [21]. In the neighbourhood of $E = -1$ the dispersion relation approaches a quadratic form, and our quadratic method yields zero error. The Van Hove singularity

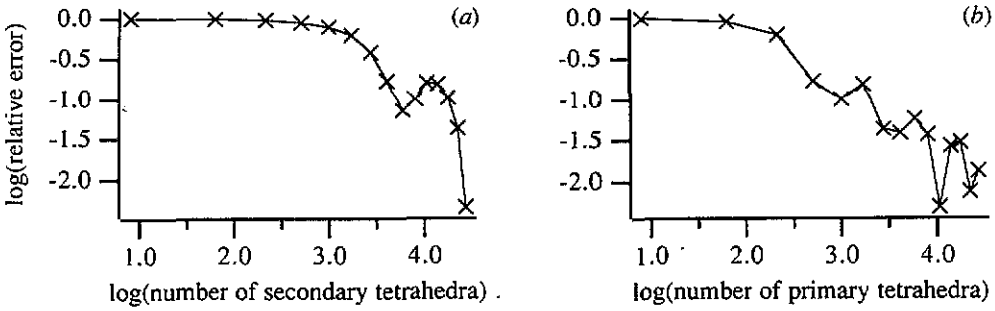

Figure 3. (*a*) Convergence of the density of states with the number of secondary tetrahedra if the quadratic surface is the sphere $x^2 + y^2 + z^2 = 0.005$ and the primary tetrahedron is $(0, 0, 0)$, $(1, 0, 0)$, $(0, 1, 0)$, $(0, 0, 1)$. (*b*) Convergence of density of states in the 'standard' HTM with the number of primary tetrahedra if the quadratic surface is $x^2 + y^2 + z^2 = 0.005$ and the IBZ is $(0, 0, 0)$, $(1, 0, 0)$, $(0, 1, 0)$, $(0, 0, 1)$. A primary tetrahedron is then always divided into 64 smaller tetrahedra.

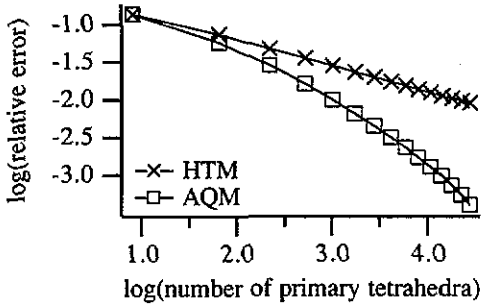

Figure 4. Convergence of the density of states with the number of primary tetrahedra for the 'standard' HTM and the AQM if the surface is $-(\cos(\pi x) + \cos(\pi y) + \cos(\pi z))/3 = -1/3$ and the IBZ is the tetrahedron $(0, 0, 0)$, $(1, 0, 0)$, $(1, 1, 0)$, $(1, 1, 1)$.

at $E = -1/3$ is not of quadratic type, but figure 4 shows that our method still gives good convergence compared to the HTM.

It is to be realized that the correct handling of the Van Hove singularities of the $\varepsilon_q(\boldsymbol{k})$ in the primary tetrahedrons is not a matter of only academic interest since such singularities occur frequently. We found for example in a moderately accurate band-structure calculation on silicon (24 primary tetrahedra in the IBZ) 47 quadratic Van Hove singularities (i.e. $|\nabla\varepsilon_q(\boldsymbol{k})| = 0$) in the four occupied valence bands.

It is clearly desirable to have a method to evaluate the surface integral $I(E)$ in three-dimensional systems exactly (i.e. to machine accuracy) while using quadratic interpolation for both $f(\boldsymbol{k})$ and $\varepsilon(\boldsymbol{k})$. The volume integral $J(E)$ can then also be done exactly according to the procedure described in appendix 2 of [20]. Such a method is presented in this paper. The method is based on a transformation of variables which allows one to deal straightforwardly with the δ-function in $I(E)$. In section 2 we demonstrate this method by applying it to the simple, commonly used linear interpolation. Numerically this yields of course the same results as the likewise exact LTM. In section 3 the problems arising in the application of the method to quadratic interpolation are discussed. It turns out that a transformation to new variables such that all integrals can be done analytically is not always possible. The solution is to resort to a numerical

integration in one variable, which can be carried out to arbitrary accuracy using standard one-dimensional numerical integration techniques. The remaining two-dimensional integral can then be done analytically by the transformation-of-variables method as already demonstrated in [20]. In section 4 we compare our method to other methods of BZ integral evaluation. In the appendices some closely related subjects are treated.

2. Linear interpolation

When using linear interpolation for $f(k)$ and $\varepsilon(k)$, we have

$$f_l(x,y,z) = p_1 + p_2x + p_3y + p_4z \qquad \varepsilon_l(x,y,z) = q_1 + q_2x + q_3y + q_4z. \tag{3}$$

The constants p_i and q_i can be found by solving a system of four linear equations in four unknowns. The integral (2) becomes

$$\int_V f(k)\delta(E - \varepsilon(k))\,\mathrm{d}k = \int_V f_l(x,y,z)\delta(E - \varepsilon_l(x,y,z))\,\mathrm{d}x\,\mathrm{d}y\,\mathrm{d}z \equiv \sum_{i=1}^{4} p_i I_i(E) \tag{4}$$

where

$$I_i(E) = \int_V \mu_i(x,y,z)\delta(E - \varepsilon_l(x,y,z))\,\mathrm{d}x\,\mathrm{d}y\,\mathrm{d}z \tag{5}$$

and $\mu_i(x,y,z) = 1, x, y, z$ for $i = 1, 2, 3, 4$. Note that $I_1(E)$ is the density of states DOS(E). So if we can evaluate the integrals $I_i(E)$, we can integrate any linear function $f_l(x,y,z)$ over the linear surface $E = \varepsilon_l(x,y,z)$. To evaluate the integral

$$\int_V \mu_i(x,y,z)\delta(E - \varepsilon_l(x,y,z))\,\mathrm{d}x\,\mathrm{d}y\,\mathrm{d}z \tag{6}$$

we make a change of variables from (x,y,z) to (e,u,v)

$$x = f(e,u,v) \qquad y = g(e,u,v) \qquad z = h(e,u,v) \tag{7}$$

such that

$$\varepsilon_l(x,y,z) = \varepsilon_l(f(e,u,v), g(e,u,v), h(e,u,v)) \equiv e. \tag{8}$$

The transformation can be seen as a parametrization of all surfaces $e = \varepsilon_l(x,y,z)$ in the parameters u and v. This transformation removes the δ-function, changing the integral from an integral in three variables (x,y,z) to an integral in two variables (u,v).

$$\begin{aligned}
&\int_{V_{x,y,z}} \mu(x,y,z)\delta(E - \varepsilon_l(x,y,z))\,\mathrm{d}x\,\mathrm{d}y\,\mathrm{d}z \\
&\quad = \int_{V_{e,u,v}} \mu_i(e,u,v)\delta(E-e)\frac{\partial(x,y,z)}{\partial(e,u,v)}\,\mathrm{d}e\,\mathrm{d}u\,\mathrm{d}v \\
&\quad = \int_{V_{u,v}(\varepsilon)} \mu_i(E,u,v)\frac{\partial(x,y,z)}{\partial(e,u,v)}\bigg|_{e=E}\,\mathrm{d}e\,\mathrm{d}u\,\mathrm{d}v
\end{aligned} \tag{9}$$

where $V_{u,v}(E)$ is the domain in (u,v) space corresponding to the part of the surface

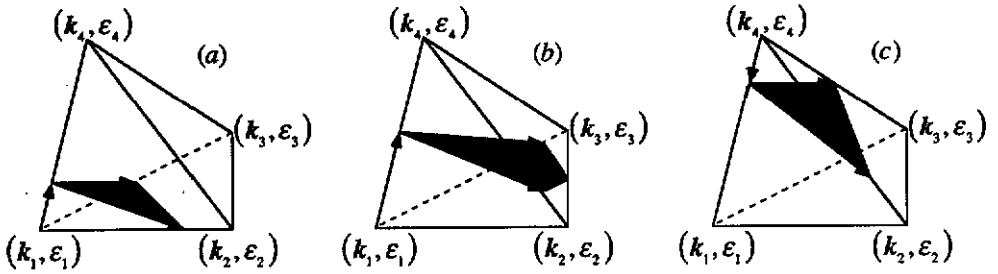

Figure 5. The vectors used for the parametrization of the linear surface $e = \varepsilon_l(x, y, z)$ (the grey-shaded plane) if (*a*) $\varepsilon_1 < E < \varepsilon_2 < \varepsilon_3 < \varepsilon_4$ (*b*) $\varepsilon_1 < \varepsilon_2 < E < \varepsilon_3 < \varepsilon_4$ and (*c*) $\varepsilon_1 < \varepsilon_2 < \varepsilon_3 < E < \varepsilon_4$.

$E = \varepsilon_l(x, y, z)$ lying within the tetrahedron. We try to find parametrizations such that the integral (9) can be done analytically.

When using linear interpolation, the surfaces $e = \varepsilon_l(x, y, z)$ are planes and parameterizations are easily given. We assume that the corners of the tetrahedron are numbered such that $\varepsilon_1 < \varepsilon_2 < \varepsilon_3 < \varepsilon_4$. Three cases have to be considered.

(i) $\varepsilon_1 < E < \varepsilon_2 < \varepsilon_3 < \varepsilon_4$. The intersection of the linear surface with the tetrahedron consists of one triangle (figure 5(*a*)).

A parametrization for the surface $e = \varepsilon_l(x, y, z)$ is

$$\boldsymbol{k} = \boldsymbol{k}_1 + \frac{e-\varepsilon_1}{\varepsilon_4-\varepsilon_1}(\boldsymbol{k}_4-\boldsymbol{k}_1) + u\left(\frac{e-\varepsilon_1}{\varepsilon_3-\varepsilon_1}(\boldsymbol{k}_3-\boldsymbol{k}_1) - \frac{e-\varepsilon_1}{\varepsilon_4-\varepsilon_1}(\boldsymbol{k}_4-\boldsymbol{k}_1)\right) + v\left(\frac{e-\varepsilon_1}{\varepsilon_2-\varepsilon_1}(\boldsymbol{k}_2-\boldsymbol{k}_1) - \frac{e-\varepsilon_1}{\varepsilon_4-\varepsilon_1}(\boldsymbol{k}_4-\boldsymbol{k}_1)\right) \tag{10}$$

where $0 \leqslant u \leqslant 1$, $0 \leqslant v \leqslant 1-u$. The Jacobian is

$$\frac{\partial(x,y,z)}{\partial(e,u,v)} = \frac{(e-\varepsilon_1)^2}{(\varepsilon_4-\varepsilon_1)(\varepsilon_3-\varepsilon_1)(\varepsilon_2-\varepsilon_1)}V \tag{11}$$

with

$$V = \begin{vmatrix} k_{2x}-k_{1x} & k_{3x}-k_{1x} & k_{4x}-k_{1x} \\ k_{2y}-k_{1y} & k_{3y}-k_{1y} & k_{4y}-k_{1y} \\ k_{2z}-k_{1z} & k_{3z}-k_{1z} & k_{4z}-k_{1z} \end{vmatrix} \tag{12}$$

which is six times the volume of the tetrahedron.

(ii) $\varepsilon_1 < \varepsilon_2 < E < \varepsilon_3 < \varepsilon_4$. The intersection of the linear surface with the tetrahedron consists of a quadrangle (two triangles) (figure 5(*b*)). For one triangle a parametrization is

$$\boldsymbol{k} = \boldsymbol{k}_1 + \frac{e-\varepsilon_1}{\varepsilon_4-\varepsilon_1}(\boldsymbol{k}_4-\boldsymbol{k}_1) + u\left(\frac{e-\varepsilon_1}{\varepsilon_3-\varepsilon_1}(\boldsymbol{k}_3-\boldsymbol{k}_1) - \frac{e-\varepsilon_1}{\varepsilon_4-\varepsilon_1}(\boldsymbol{k}_4-\boldsymbol{k}_1) + v\left((\boldsymbol{k}_2-\boldsymbol{k}_1) + \frac{e-\varepsilon_2}{\varepsilon_3-\varepsilon_2}(\boldsymbol{k}_3-\boldsymbol{k}_2) - \frac{e-\varepsilon_1}{\varepsilon_4-\varepsilon_1}(\boldsymbol{k}_4-\boldsymbol{k}_1)\right)\right). \tag{13}$$

The Jacobian is

$$\frac{\partial(x,y,z)}{\partial(e,u,v)} = \frac{(e-\varepsilon_1)(\varepsilon_3-e)}{(\varepsilon_4-\varepsilon_1)(\varepsilon_3-\varepsilon_1)(\varepsilon_3-\varepsilon_2)} V. \tag{14}$$

And for the other triangle:

$$\boldsymbol{k} = \boldsymbol{k}_1 + \frac{e-\varepsilon_1}{\varepsilon_4-\varepsilon_1}(\boldsymbol{k}_4-\boldsymbol{k}_1) + u\left((\boldsymbol{k}_2-\boldsymbol{k}_1) + \frac{e-\varepsilon_2}{\varepsilon_4-\varepsilon_2}(\boldsymbol{k}_4-\boldsymbol{k}_2) - \frac{e-\varepsilon_1}{\varepsilon_4-\varepsilon_1}(\boldsymbol{k}_4-\boldsymbol{k}_1)\right)$$
$$+ v\left((\boldsymbol{k}_2-\boldsymbol{k}_1) + \frac{e-\varepsilon_2}{\varepsilon_3-\varepsilon_2}(\boldsymbol{k}_3-\boldsymbol{k}_2) - \frac{e-\varepsilon_1}{\varepsilon_4-\varepsilon_1}(\boldsymbol{k}_4-\boldsymbol{k}_1)\right) \tag{15}$$

with the Jacobian

$$\frac{\partial(x,y,z)}{\partial(e,u,v)} = \frac{(e-\varepsilon_2)(\varepsilon_4-e)}{(\varepsilon_4-\varepsilon_2)(\varepsilon_3-\varepsilon_2)(\varepsilon_4-\varepsilon_1)} V. \tag{16}$$

(iii) $\varepsilon_1 < \varepsilon_2 < \varepsilon_3 < E < \varepsilon_4$. This resembles case (i). The intersection of the linear surface with the tetrahedron consists of one triangle (figure 5(*c*)) with parametrization

$$\boldsymbol{k} = \boldsymbol{k}_4 + \frac{e-\varepsilon_4}{\varepsilon_4-\varepsilon_1}(\boldsymbol{k}_4-\boldsymbol{k}_1) + u\left(\frac{e-\varepsilon_4}{\varepsilon_4-\varepsilon_3}(\boldsymbol{k}_4-\boldsymbol{k}_3) - \frac{e-\varepsilon_4}{\varepsilon_4-\varepsilon_1}(\boldsymbol{k}_4-\boldsymbol{k}_1)\right)$$
$$+ v\left(\frac{e-\varepsilon_4}{\varepsilon_4-\varepsilon_2}(\boldsymbol{k}_4-\boldsymbol{k}_2) - \frac{e-\varepsilon_4}{\varepsilon_4-\varepsilon_1}(\boldsymbol{k}_4-\boldsymbol{k}_1)\right). \tag{17}$$

The Jacobian is

$$\frac{\partial(x,y,z)}{\partial(e,u,v)} = \frac{(e-\varepsilon_4)^2}{(\varepsilon_4-\varepsilon_1)(\varepsilon_4-\varepsilon_2)(\varepsilon_4-\varepsilon_3)} V. \tag{18}$$

In all cases, the transformations have the form

$$\begin{cases} x = t_x(E) + uu_x(E) + vv_x(E) \\ y = t_y(E) + uu_y(E) + vv_y(E) \\ z = t_z(E) + uu_z(E) + vv_z(E) \end{cases} \qquad \frac{\partial(x,y,z)}{\partial(e,u,v)} = D(E). \tag{19}$$

The integrals become

$$I_1 = \int_V \delta(E-\varepsilon_l(x,y,z))\,\mathrm{d}x\,\mathrm{d}y\,\mathrm{d}z = D\int_0^1 \mathrm{d}u \int_0^{1-u} \mathrm{d}v = \frac{D}{2} \tag{20a}$$

$$I_2 = \int_V x\delta(E-\varepsilon_l(x,y,z))\,\mathrm{d}x\,\mathrm{d}y\,\mathrm{d}z = D\int_0^1 \mathrm{d}u \int_0^{1-u} \mathrm{d}v\,(t_x + uu_x + vv_x)$$
$$= \frac{(3t_x + u_x + v_x)}{6} D \tag{20b}$$

$$I_3 = \int_V y\delta(E-\varepsilon_l(x,y,z))\,\mathrm{d}x\,\mathrm{d}y\,\mathrm{d}z = D\int_0^1 \mathrm{d}u \int_0^{1-u} \mathrm{d}v\,(t_y + uu_y + vv_y)$$
$$= \frac{(3t_y + u_y + v_y)}{6} D \tag{20c}$$

Table 2. The various forms to which a quadratic surface can be reduced and the types of surfaces they represent. All constants q_i ($i = 2, \ldots, 9$) are non-zero.

Surface	Type
$\varepsilon = q_1 + q_5x^2 + q_8y^2 + q_{10}z^2$	ellipsoid (q_5, q_8, q_{10} the same sign)
$\varepsilon = q_1 + q_5x^2 + q_8y^2 + q_{10}z^2$	hyperboloid of one or two sheets (q_5, q_8, q_{10} not the same sign)
$\varepsilon = q_1 + q_4z + q_5x^2 + q_8y^2$	elliptic paraboloid (q_5 and q_8 the same sign)
$\varepsilon = q_1 + q_4z + q_5x^2 + q_8y^2$	hyperbolic paraboloid (q_5 and q_8 not the same sign)
$\varepsilon = q_1 + q_5x^2 + q_8y^2$	elliptic cylinder (q_5 and q_8 the same sign)
$\varepsilon = q_1 + q_5x^2 + q_8y^2$	hyperbolic cylinder (q_5 and q_8 not the same sign)
$\varepsilon = q_1 + q_3y + q_5x^2$	parabolic cylinder
$\varepsilon = q_1 + q_2x$	plane
$\varepsilon = q_1 + q_5x^2$	degenerate (two parallel planes)
$\varepsilon = q_1$	degenerate

$$I_4 = \int_V z\delta(E - \varepsilon_i(x, y, z))\,dx\,dy\,dz = D\int_0^1 du \int_0^{1-u} dv\,(t_z + uu_z + vv_z)$$

$$= \frac{(3t_z + u_z + v_z)}{6} D. \tag{20d}$$

We conclude that the transformation of integration variables leads by direct algebraic manipulation to the equations of the linear tetrahedron method.

3. Quadratic interpolation

When using quadratic interpolation for the functions $f(\boldsymbol{k})$ and $\varepsilon(\boldsymbol{k})$, we have

$$f_q(x, y, z) = p_1 + p_2x + p_3y + p_4z + p_5x^2 + p_6xy + p_7xz + p_8y^2 + p_9yz + p_{10}z^2 \tag{21}$$

$$\varepsilon_q(x, y, z) = q_1 + q_2x + q_3y + q_4z + q_5x^2 + q_6xy + q_7xz + q_8y^2 + q_9yz + q_{10}z^2. \tag{22}$$

The constants p_i and q_i can be found by solving a system of ten equations in ten unknowns (see figure 1). The integral (2) becomes

$$\int_V f(\boldsymbol{k})\delta(E - \varepsilon(\boldsymbol{k}))\,d\boldsymbol{k} = \int_V f_q(x, y, z)\delta(E - \varepsilon_q(x, y, z))\,dx\,dy\,dz \equiv \sum_{i=1}^{10} p_i I_i(E) \tag{23}$$

where

$$I_i(E) = \int_V \mu_i(x, y, z)\delta(E - \varepsilon_q(x, y, z))\,dx\,dy\,dz \tag{24}$$

and $\mu_i(x, y, z) = 1, x, y, z, x^2, xy, xz, y^2, yz, z^2$ for $i = 1, 2, \ldots, 10$. So if we can evaluate the integrals $I_i(E)$, we can integrate any quadratic function $f_q(x, y, z)$ over the quadratic surface $E = \varepsilon_q(x, y, z)$. If we apply an affine transformation

$$\boldsymbol{k} = \mathbf{A}\boldsymbol{k}' + \boldsymbol{b} \tag{25}$$

to the integrals (23), the functions $f_q(\boldsymbol{k})$ and $\varepsilon_q(\boldsymbol{k})$ remain quadratic functions and the volume of integration remains a tetrahedron. It is well known [22] that there always exists an affine transformation such that $\varepsilon_q(\boldsymbol{k})$ takes one of the forms given in table 2.

If the coefficients q_5, q_8 and q_{10} are non-zero (which is generally the case) and have the same sign the surface is an ellipsoid. For all other combinations of signs the surface is a hyperboloid of one or two sheets. According to our experience practically only the ellipsoid (about 25% of all cases) and the hyperboloid of one or two sheets (about 75% of all cases) occur.

Let us first try to follow the same procedure as for the linear approximation in the previous section and for the two-dimensional quadratic case in [20]. We make a change of variables from (x, y, z) to (e, u, v)

$$x = f(e, u, v) \qquad y = g(e, u, v) \qquad z = h(e, u, v) \tag{26}$$

such that

$$\varepsilon_q(x, y, z) = \varepsilon_q(f(e, u, v), g(e, u, v), h(e, u, v)) \equiv e. \tag{27}$$

This transformation can be seen as a parametrization of all surfaces $e = \varepsilon_q(x, y, z)$ in the parameters u and v. This transformation removes the δ-function

$$\begin{aligned}\int_{V_{x,y,z}} \mu_i(x, y, z)\delta(E - \varepsilon_q(x, y, z))\,\mathrm{d}x\,\mathrm{d}y\,\mathrm{d}z \\ = \int_{V_{e,u,v}} \mu_i(e, u, v)\delta(E - e)\frac{\partial(x, y, z)}{\partial(e, u, v)}\,\mathrm{d}e\,\mathrm{d}u\,\mathrm{d}v \\ = \int_{V_{u,v}(E)} \mu_i(E, u, v)\frac{\partial(x, y, z)}{\partial(e, u, v)}\bigg|_{e=E}\,\mathrm{d}u\,\mathrm{d}v.\end{aligned} \tag{28}$$

For the elliptic cylinder (see appendix 1), the hyperbolic cylinder, the parabolic cylinder, the plane and the two degenerate cases parametrizations can be found such that integral (28) can be done analytically. However, we have not been able to find such parametrizations for the ellipsoid, the hyperboloid of one or two sheets, the elliptic paraboloid or the hyperbolic paraboloid. As an example of the problems involved, we consider a simple case: the DOS(E) if the quadratic surface is the sphere $E = x^2 + y^2 + z^2$. A possible parametrization for the surface of the sphere $E = x^2 + y^2 + z^2$ is the one corresponding to spherical polar coordinates $(u = \theta, v = \phi)$

$$\begin{cases} x = \sqrt{E}\sin(u)\cos(v) \\ y = \sqrt{E}\sin(u)\sin(v) \\ z = \sqrt{E}\cos(v) \end{cases} \qquad \frac{\partial(x, y, z)}{\partial(e, u, v)} = \tfrac{1}{2}\sqrt{E}\sin(u). \tag{29}$$

If the energy is such that the sphere $E = x^2 + y^2 + z^2$ lies entirely within the tetrahedron (figure 6(a)), the limits on the u integral are 0 and π, and on the v integral 0 and 2π. The DOS(E) becomes

$$\int_0^{\pi} \mathrm{d}u \int_0^{2\pi} \mathrm{d}v\, \tfrac{1}{2}\sqrt{E}\sin(u) = 2\pi\sqrt{E}, \tag{30}$$

the normal $\sqrt{E}$ form of the DOS(E) if the dispersion relation is perfectly spherical. However, when the sphere $E = x^2 + y^2 + z^2$ cuts the faces, or faces and edges, of the tetrahedron (figure 6(b)), the domain in u, v-space (using the parametrization (29)) is very complicated and analytical evaluation of the integrals (28) is difficult, if not impossible.

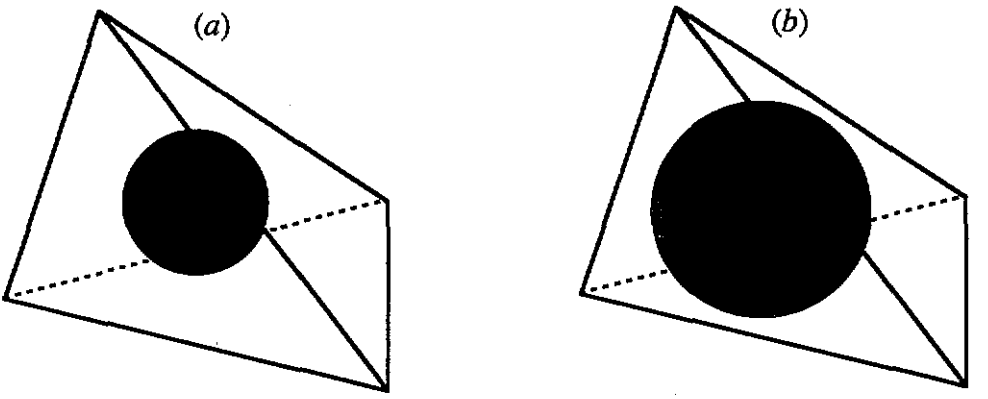

Figure 6. Examples of intersections of a sphere with a tetrahedron. In (*a*) the sphere lies entirely within the tetrahedron, in (*b*) the sphere cuts a face of the tetrahedron.

Compared to this 'simple' example, there is a large variety of more complicated situations, considering all the forms of quadratic surfaces that may occur as well as their positions with respect to the tetrahedron. Given the very complicated domains in u, v-space that will result, there is very little hope indeed of finding for each case a u, v-parametrization that would make analytical evaluation of the integral possible. The complicated domains in u, v-space also make highly accurate two-dimensional numerical integration in u and v impossible. (Incidentally, figure 6 provides very direct insight in the deficiency of the linear approximation. Suppose ε_1 is the lowest energy at a corner and ε_4 the highest. The sphere $E = x^2 + y^2 + z^2$ thus cuts for the first time through a corner of the tetrahedron at $E = \varepsilon_1$. The linear tetrahedron method will give a DOS equal to zero, i.e. a 100% error, for all energies between zero and ε_1. This is because any energy below ε_1 or above ε_4 will in a linear approximation automatically fall outside the tetrahedron's range of energies (see also appendix 2).)

In order to evaluate $I_i(E)$ accurately when using quadratic interpolation, we proceed as follows. The integrals (24) are rewritten as the iterated integrals

$$\int_{z_{\min}}^{z_{\max}} \mathrm{d}z \int_{V_{x,y}(z)} \mathrm{d}x\,\mathrm{d}y\,\mu_i(x,y,z)\delta(E-\varepsilon_q(x,y,z)) \equiv \int_{z_{\min}}^{z_{\max}} I_i(z,E)\,\mathrm{d}z \qquad (31)$$

where $z_{\min}$ and $z_{\max}$ are the minimum and maximum z-coordinates of the corners of the tetrahedron. At a specific z the inner integral over x and y is just the quadratic two-dimensional Brillouin zone integral that we solved [20]. For constant z, $V_{x,y}(z)$ is the intersection of the plane $z =$ constant with the tetrahedron and consists of either a triangle or a quadrangle (i.e. two adjacent triangles) (figure 7(*a*)) and thus corresponds to a triangular (quadrangular) two-dimensional Brillouin zone. Also, for constant z, $\varepsilon_q(x, y, z)$ is a quadratic function in x and y in the plane $z =$ constant and $E = \varepsilon_q(x, y, z)$ is a quadratic curve in that plane: an ellipse, a hyperbola, a parabola, or a straight line (figure 7(*b*)). The inner integral $I_i(z, E)$ is thus the integral over the parts of a quadratic curve lying within a triangle that was treated in [20]. Using the results of [20] for the inner integral we are left with the outer z-integration.

By way of illustration, we consider again the DOS(E) if the surface $E = x^2 + y^2 + z^2$ lies entirely within the tetrahedron. On the intervals $z_{\min} \leqslant z < -\sqrt{E}$ and $\sqrt{E} < z \leqslant z_{\max}$ the planes $z =$ constant do not cut the sphere, the contribution to the integral is

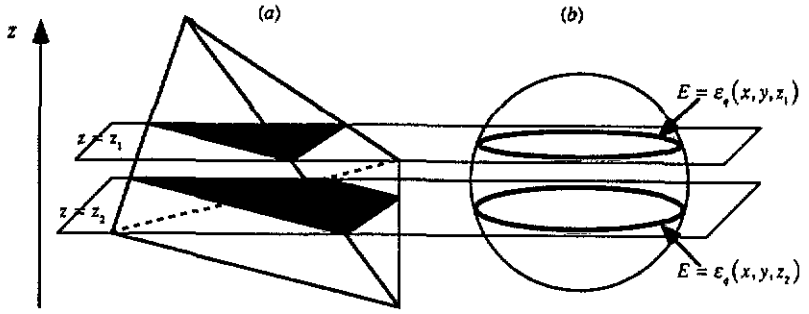

Figure 7. (*a*) The intersections of planes z = constant with a tetrahedron consist of one or two triangles. (*b*) The intersections of planes z = constant with quadratic surface (here a sphere) consist of quadratic curves (here circles).

zero and we may take as limits on the z-integral $-\sqrt{E}$ and $\sqrt{E}$. The intersections of the planes z = constant with the sphere and the tetrahedron consist of circles lying entirely within the triangles (quadrangles). We showed [20] that for this case the integral $I_1(z, E)$ is equal to π (and is accidentally not z-dependent), so the DOS(E) becomes

$$\int_{z_{\min}}^{z_{\max}} \mathrm{d}z \int_{V_{x,y}(z)} \mathrm{d}x\,\mathrm{d}y\,\delta(E - \varepsilon_q(x, y, z)) = \int_{-\sqrt{E}}^{\sqrt{E}} \mathrm{d}z\,\pi = 2\pi\sqrt{E} \tag{32}$$

leading, of course, to the previous result (30).

However, when the sphere cuts the faces, or the faces and the edges, of the tetrahedron (figure 6(*b*)) the integral over z is not easily evaluated analytically. We could use some standard one-dimensional numerical integration (e.g. Gauss–Legendre) for the z-integral

$$\int_{z_{\min}}^{z_{\max}} \mathrm{d}z \int_{V_{x,y}(z)} \mathrm{d}x\,\mathrm{d}y\,f_q(x, y, z)\delta(E - \varepsilon_q(x, y, z))$$

$$\approx \sum_{i=1}^{N_z} w(z_i) \int_{V_{x,y}(z_i)} \mathrm{d}x\,\mathrm{d}y\,f_q(x, y, z_i)\delta(E - \varepsilon_q(x, y, z_i)) \tag{33}$$

where z_i and $w(z_i)$ are the nodes and weights of the integration formula, respectively. At each z_i, the two-dimensional integral $I(z_i, E)$ is solved with the method (and routines) of [20]. Unfortunately, the numerical integration over the entire z-interval shows poor convergence because of singularities (discontinuous derivatives) in the function $I(z, E)$ for z-coordinates where the quadratic surface cuts the faces or the edges of the tetrahedron (figure 8). The calculation of these z-coordinates is straightforward, but tedious.

For accurate numerical integration, we have to partition the z-interval into intervals with the singularities at the endpoints

$$\int_{z_{\min}}^{z_{\max}} I_i(z, E)\,\mathrm{d}z \approx \sum_{j=1}^{N-1} \int_{z_j}^{z_{j+1}} I_i(z, E)\,\mathrm{d}z \tag{34}$$

and apply a simple transformation to each z-interval to remove the endpoint singu-

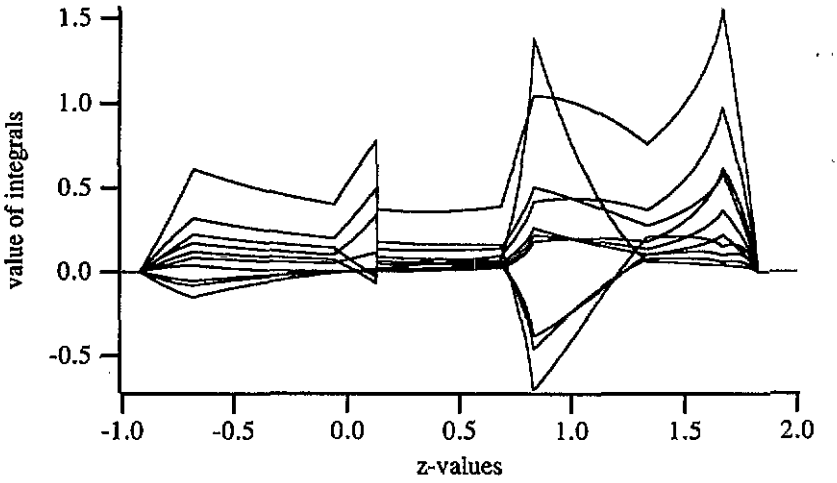

Figure 8. The z-dependence of the ten integrals $I_i(z, E)$ in case the quadratic surface is the sphere $x^2 + y^2 + z^2 = 10$ and the coordinates of the corners of the tetrahedron are $(1, 3, 2)$, $(-3, 2, 1)$, $(-2, -3, 0)$ and $(2, 3, -1)$. Singularities occur at approximately -1.00, -0.92, -0.68, -0.062, 0.13, 0.68, 0.83, 1.33, 1.67, 1.82, and 2.00.

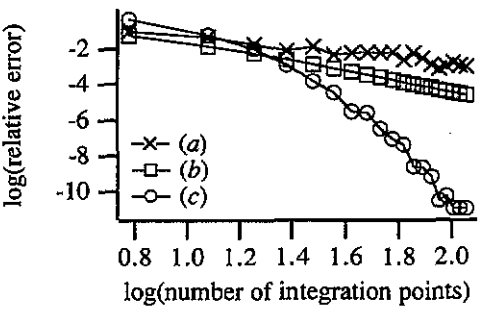

Figure 9. Convergence of various methods to evaluate the integral (31) numerically. (*a*) Straightforward integration over the whole z-interval, (*b*) division of the whole z-interval in subintervals with the singularities at the endpoints and (*c*) division of the whole z-interval in subintervals with the singularities at the endpoints *and* application of the transformation (35) to each subinterval.

larities. The transformation

$$z = \left[1 + \sin\left(\frac{\pi}{2}z'\right)\right]\frac{z_{j+1} - z_j}{2} + z_j \qquad -1 \leq z' \leq 1 \tag{35}$$

appears to work well in practice. In figure 9 a typical example is given of the convergence of the numerical integration without division in intervals (figure 9(*a*)), with division in intervals (figure 9(*b*)) and division in intervals and transformation (figure 9(*c*)). Clearly, for high accuracy method (*c*) is the one to be used. Gauss–Legendre integration is used for each interval.

As a final remark we note that the volume integral $J(E)$ can be obtained from the surface integral $I(E)$ by the procedure described in appendix 2 of [20]. For this procedure it is essential that we can calculate the minimum energy $\varepsilon_{\min}$ and the maximum energy $\varepsilon_{\max}$ of $\varepsilon_q(\boldsymbol{k})$, where $\boldsymbol{k}$ varies over the tetrahedron. As knowledge of these energies increases the efficiency of the method considerably (if we know that $E < \varepsilon_{\min}$ or $E > \varepsilon_{\max}$

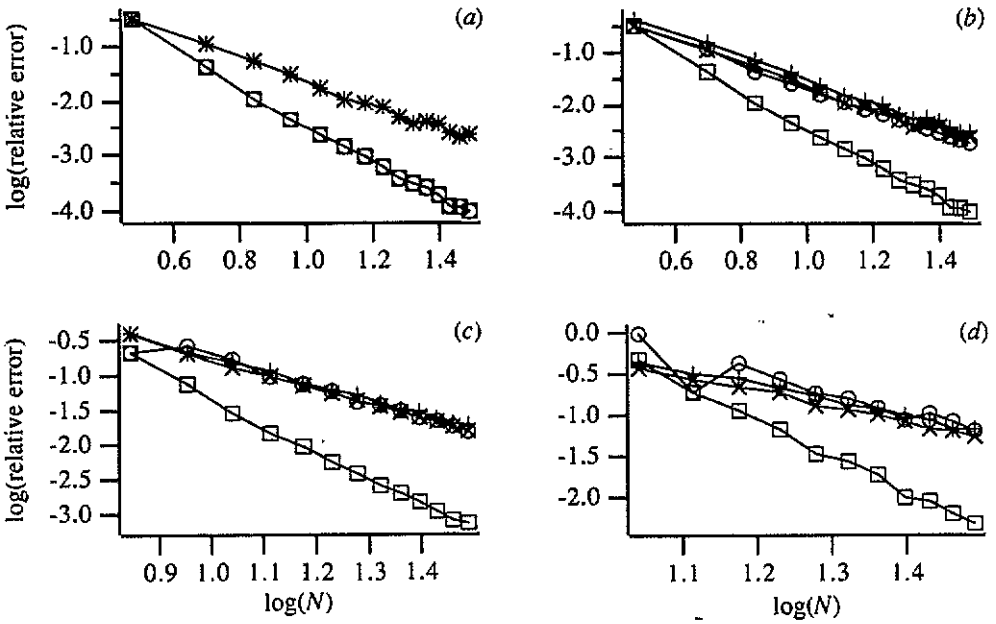

Figure 10. Convergence behaviour of the integrals (36) for various approximations (constant (c), linear (l), quadratic (q)) of $f(k)$ and $\varepsilon(k)$. + cl; × ll; ○ lq; □ qq; (*a*) $f(k) = 1$; (*b*) $f(k) = \cos(\pi x) + \cos(\pi y) + \cos(\pi z)$; (*c*) $f(k) = \cos(3\pi x) + \cos(3\pi y) + \cos(3\pi z)$; (*d*) $f(k) = \cos(6\pi x) + \cos(6\pi y) + \cos(6\pi z)$.

the surface integral $I(E)$ is zero) and is also of great practical utility (e.g. to narrow down the energy-interval that has to be searched for the Fermi energy) we discuss the calculation of $\varepsilon_{\min}$ and $\varepsilon_{\max}$ in some detail in appendix 2.

We conclude that the proposed scheme is capable of 'exact' evaluation of the Brillouin zone integrals $I(E)$ and $J(E)$ with quadratically interpolated $f(k)$ and $\varepsilon(k)$.

4. Results and discussion

We test our method by calculating the tight binding Green's function integrals

$$\int_{-1}^{1}\int_{-1}^{1}\int_{-1}^{1} \mathrm{d}x\,\mathrm{d}y\,\mathrm{d}z(\cos(n\pi x) + \cos(n\pi y) + \cos(n\pi z))\delta\{E + \tfrac{1}{3}[\cos(\pi x) + \cos(\pi y) + \cos(\pi z)]\} \tag{36}$$

for an increasing number of k-points along the edge of the irreducible wedge (denoted by N) for various methods listed in table 1 (figure 10). N must of course be large enough to resolve the oscillations of the functions $\varepsilon(k)$ and $f(k)$. A reasonable minimum seems one plus the number of extrema of these functions along an edge of the IW.

The following abbreviations are used: (cl): constant interpolation for $f(k)$, linear interpolation for $\varepsilon(k)$; (ll): linear interpolation for both $f(k)$ and $\varepsilon(k)$; (lq): linear interpolation for $f(k)$, quadratic interpolation for $\varepsilon(k)$; (qq): quadratic interpolation for both $f(k)$ and $\varepsilon(k)$.

The integrals were evaluated for 100 evenly spaced energies in the range $[-1, 1]$ and the root mean square deviation from the exact (converged) result was determined. All

Table 3. Comparison of the exponents β in (37) for the various methods used to evaluate the integrals (36).

	(*a*)	(*b*)	(*c*)	(*d*)
(cl)	2.2	2.2	2.0	1.9
(ll)	2.2	2.2	2.1	1.9
(lq)	3.4	2.2	2.0	2.2
(qq)	3.4	3.4	3.8	4.4

methods used the same number of k-points, which was accomplished by a division of the tetrahedra in which the (lq) and (qq) were carried out into eight smaller tetrahedra in which the (cl) and (ll) integration were performed (see figure 1). Since only very few of the energies are close to the Van Hove singularities at $E = -1$ and $E = -1/3$, the present results provide information on the behaviour of the various schemes at general energies rather than that at (or close to) Van Hove energies.

Considering first figure 10(*a*) with $f(k) = 1$ (the density of states), the curves for (cl) and (ll) coincide, as do those for (lq) and (qq), because the approximation for $f(k)$ (c, l or q) is irrelevant for constant $f(k)$. Figure 10(*a*) clearly demonstrates the superiority of the quadratic approximation to $\varepsilon(k)$, in agreement with the findings of Methfessel *et al* [17–19]. All methods give the same RMS error in figure 10(*a*) when N equals 3, because the quadratically interpolated $\varepsilon(k)$ is then accidentally linear. Considering next figure 10(*b*), $(f(k) = \cos(\pi x) + \cos(\pi y) + \cos(\pi z))$, we note that the (qq) method is superior, as expected. It is surprising that the (lq) method is doing so poorly, in particular also with respect to the linear method (ll), but this is due to the fact that the (lq) method, for consistency with the approach of Methfessel *et al* [19] uses a linear (least squares) approximation of $f(k)$ in the large tetrahedra, which have k-points at the corners and the midpoints of the edges, whereas the (ll) method uses a separate linear interpolation in each of the eight smaller tetrahedra into which a large tetrahedron may be subdivided (see figure 1). Apparently, the advantage of a finer division in the (ll) method, for the same k-point density, outweighs the advantage of the quadratic interpolation of $\varepsilon(k)$ in the (lq) method. (The phenomenon of different methods giving an identical log(RMS) at particular values of N, due to accidental linear behaviour of the quadratic interpolation, occurs in each case: in figure 10(*b*) (ll), (lq) and (qq) coincide at $N = 3$ because both $f(k)$ and $\varepsilon(k)$ are linear; in figure 10(*c*) (lq) and (qq) coincide at $N = 7$, because $f(k)$ is linear. In figure 10(*d*) this happens at $N = 13$.)

As has been found for the two-dimensional case, the (qq) integration shows considerably better convergence characteristics than all other methods. The difference with the other methods is particularly striking when the function $f(k)$ varies more rapidly. This may be analyzed more quantitatively. The almost linear dependence of log(RMS) on log(N) implies that the error behaves as:

$$\text{RMS}(N) = \alpha N^{-\beta}. \tag{37}$$

It is interesting to compare the exponents β for the various methods to evaluate the integrals, since these directly reflect the convergence rate (table 3). Roughly, the exponents β are twice as large for the quadratic integration as for the commonly used linear integration. So, to achieve the same accuracy with quadratic integration as with linear integration, in the limit of large N only about the square root of the number of k-points along an edge of the IW are needed. This is not quite true for the density of states

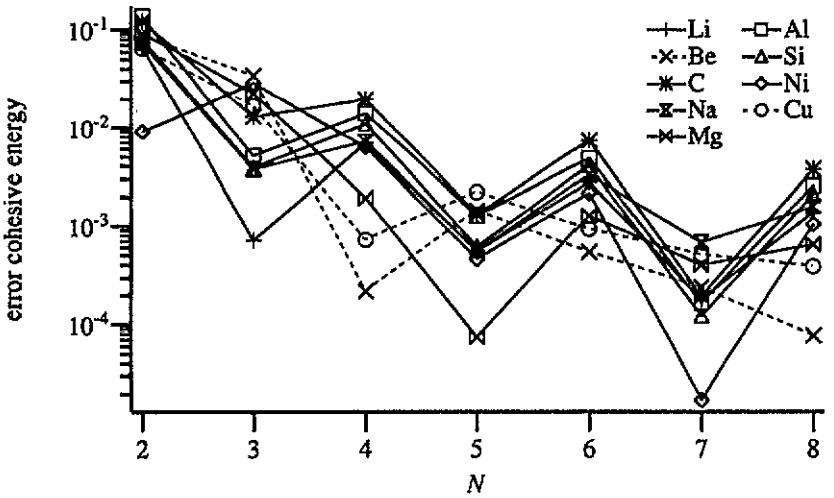

Figure 11. Convergence of the cohesive energy with the number of kH points along an edge of the irreducible wedge (denoted by N) for a number of elements. Linear interpolation was used for N even, quadratic interpolation was used for N odd.

(column (*a*)) but it definitely is for rapidly varying $f(k)$ (columns (*c*) and (*d*)). The major improvement occurs in going to (qq). The advantage will be less favourable near band crossings of course, but there is no reason to assume that the quadratic integration will be worse than the linear in such cases. Table 3 also demonstrates that an lq method [19] is a significant improvement over ll for the density of states (column (*a*)), but not for any of the integrals involving property functions (columns (*b*), (*c*) and (*d*)).

The present quadratic tetrahedron method has been implemented in a self-consistent bandstructure program [23]. Since the program does not use shape approximations to the potentials, it is possible to calculate reliable cohesive energies (for other computational details we refer to [23]). As a further illustration of the performance of the quadratic method, we show in figure 11 the convergence of the cohesive energy with the number of k-points along the edge of the irreducible wedge (denoted by N. The total number of k-points used in the calculation scales like $N^3/6$) for a number of elements. We can choose between linear or quadratic interpolation for N odd (see figure 1), but we used of course the quadratic method. For N even we must use the linear method.

We took the cohesive energy for $N = 9$ as the converged result. The error in the cohesive energy for $N = 9$ was less than or equal to 10^{-4} for all elements. This was checked for sodium, manganese and copper by calculating the cohesive energy for $N = 11$.

As can be seen from figure 11, the convergence of the cohesive energy is far better with the quadratic method than with the linear method: going from an odd N (quadratic method) to $N + 1$ (even; linear method), the error increases about an order of magnitude in spite of the larger number of k-points. Only beryllium and copper behave anomalously. The quadratic method with $N = 5$ gives an average error in the cohesive energy of 9.3×10^{-4}. The linear method needs $N = 8$ (which means a threefold increase of the number of k-points used in the calculation) to achieve the same accuracy (the average error for $N = 8$ is 1.5×10^{-3}). For beryllium and copper the quadratic method with $N = 5$ gives worse results than the linear method with $N = 4$, but it is not the quadratic method giving a larger error than expected (the errors for $N = 5$ are 1.4×10^{-3} for beryllium and

2.2×10^{-3} for copper, compared to the average error of 9.3×10^{-4} for $N = 5$), but rather the linear method giving an error much smaller than expected (the errors for $N = 4$ are 2.1×10^{-4} for beryllium and 7.1×10^{-4} for copper, compared to the average error of 7.5×10^{-3}). The errors for $N = 4$ are even smaller than for $N = 6$.

The rate of convergence of the cohesive energy is also far better for the quadratic than for the linear method: the exponent β is 2.3 for the linear method and 4.8 for the quadratic method (compare table 3). So here too we find that when the quadratic method is compared to the linear method, far fewer $\boldsymbol{k}$-points are necessary to obtain a desired accuracy.

5. Summary and conclusions

We have introduced a new method for the accurate evaluation of the surface integral $I(E)$ and the volume integral $J(E)$ using quadratic interpolation for both the property function $f(\boldsymbol{k})$ and the dispersion relation $\varepsilon(\boldsymbol{k})$. It is well known that quadratic interpolation is essential for energies close to a Van Hove singularity, but we have stressed that it is imperative to evaluate the resulting integrals to high accuracy. The advantage of the present method over other methods of integral approximation is that the integrals can be accurately calculated in reasonable computer time. Indeed, the approach is based on a 'machine accuracy' evaluation of the integrals and may therefore be regarded as equivalent to a truly analytic evaluation of the integrals. As has been found before for the two-dimensional case, quadratic interpolation is far better than linear interpolation, in the sense that far fewer $\boldsymbol{k}$-points are needed to obtain a desired accuracy for the integrals. In particular the results presented show that (i) quadratic interpolation of $\varepsilon(\boldsymbol{k})$ combined with 'exact' evaluation of the integrals is capable of handling Van Hove singularities in the density of states (figure 4), (ii) the method considerably improves convergence with the number of $\boldsymbol{k}$-points also at general energies and (iii) the quadratic methods' inherent speed of convergence is only achieved if also the property function $f(\boldsymbol{k})$ is quadratically interpolated (figure 10, table 3).

Appendix 1. The elliptic cylinder

For some of the quadratic forms parametrizations can be found such that the evaluation of the integrals using quadratic interpolation can be done analytically. As an example, explicit expressions for the integrals will be given in case the quadratic surface is an elliptic cylinder.

The integrals to be evaluated are

$$\int_V \mu_i(x, y, z)\delta(E - (q_1 + q_5x^2 + q_8y^2))\,\mathrm{d}x\,\mathrm{d}y\,\mathrm{d}z \tag{A1.1}$$

where $\mu_I(x, y, z) = 1, x, y, z, x^2, xy, xz, y^2, yz, z^2$ for $i = 1, 2, \ldots, 10$. We parametrize the surface by the transformation

$$\begin{cases} x = \sqrt{\dfrac{e - q_1}{q_5}}\cos(u) \\ y = \sqrt{\dfrac{e - q_1}{q_8}}\sin(u) \\ z = v. \end{cases} \qquad \frac{\partial(x, y, z)}{\partial(e, u, v)} = \frac{1}{2\sqrt{q_5q_8}} \tag{A1.2}$$

The faces of the tetrahedron can be given in the form

$$n_{jx}x + n_{jy}y + n_{jz}z = c_j \qquad (j = 1, 2, 3, 4) \tag{A1.3}$$

where $\boldsymbol{n}_j$ is a vector normal to face j of the tetrahedron. The domain in (u, v) space will be bounded by functions of the form

$$v = \frac{c_j}{n_{jz}} - \frac{n_{jx}}{n_{jz}}\sqrt{\frac{e-q_1}{q_5}}\cos(u) - \frac{n_{jy}}{n_{jz}}\sqrt{\frac{e-q_1}{q_8}}\sin(u). \tag{A1.4}$$

From (A1.4) it is clear that the integrals can be evaluated as the iterated integrals

$$\int_{V_u(E)} \mathrm{d}u \int_{f_1(E)+f_2(E)\cos(u)+f_3(E)\sin(u)}^{g_1(E)+g_2(E)\cos(u)+g_3(E)\sin(u)} \mathrm{d}v\, \mu_i(E, u, v)\frac{1}{2\sqrt{q_5 q_8}}. \tag{A1.5}$$

Explicit expressions for the integrals are as follows (for clarity, the energy dependence is dropped and the Jacobian is not included):

$$I_1 = h_1 u - h_3\cos(u) + h_2\sin(u) \tag{A1.6a}$$

$$I_2 = \tfrac{1}{2}h_2 u - \tfrac{1}{2}h_3\cos^2(u) + h_1\sin(u) + \tfrac{1}{2}h_2\cos(u)\sin(u) \tag{A1.6b}$$

$$I_3 = \tfrac{1}{2}h_3 u - h_1\cos(u) - \tfrac{1}{2}h_2\cos^2(u) - \tfrac{1}{2}h_3\cos(u)\sin(u) \tag{A1.6c}$$

$$I_4 = (\tfrac{1}{2}h_1^2 + \tfrac{1}{4}h_2^2 + \tfrac{1}{4}h_3^2)u - h_1h_3\cos(u) - \tfrac{1}{2}h_2h_3\cos^2(u) + h_1h_2\sin(u) + (\tfrac{1}{4}h_2^2 - \tfrac{1}{4}h_3^2)\cos(u)\sin(u) \tag{A1.6d}$$

$$I_5 = \tfrac{1}{2}h_1 u - \tfrac{1}{3}h_3\cos^3(u) + \tfrac{2}{3}h_2\sin(u) + \tfrac{1}{2}h_1\cos(u)\sin(u) + \tfrac{1}{3}h_2\cos^2(u)\sin(u) \tag{A1.6e}$$

$$I_6 = -\tfrac{1}{2}h_1^2\cos^2(u) - \tfrac{1}{3}h_2\cos^3(u) + \tfrac{1}{3}h_3\sin^3(u) \tag{A1.6f}$$

$$I_7 = \tfrac{1}{2}h_1h_2 u - \tfrac{1}{2}h_1h_3\cos^2(u) - \tfrac{1}{3}h_2h_3\cos^3(u) + (\tfrac{1}{2}h_2^2 + \tfrac{1}{3}h_2^2)\sin(u) + \tfrac{1}{6}h_2^2\cos^2(u)\sin(u) + \tfrac{1}{6}h_3^2\sin^3(u) \tag{A1.6g}$$

$$I_8 = \tfrac{1}{2}h_1 u - \tfrac{2}{3}h_3\cos(u) - \tfrac{1}{2}h_1\cos(u)\sin(u) - \tfrac{1}{3}h_3\cos(u)\sin^2(u) + \tfrac{1}{3}h_2\sin^3(u) \tag{A1.6h}$$

$$I_9 = \tfrac{1}{2}h_1h_3 u + (\tfrac{1}{2}h_1^2 + \tfrac{1}{3}h_3^2)\cos(u) - \tfrac{1}{2}h_1h_2\cos^2(u) - \tfrac{1}{6}h_2^2\cos^3(u) - \tfrac{1}{2}h_1h_3\cos(u)\sin(u) - \tfrac{1}{6}h_3^2\cos(u)\sin^2(u) + \tfrac{1}{3}h_2h_3\sin^3(u) \tag{A1.6i}$$

$$I_{10} = \tfrac{1}{3}h_1^3 + \tfrac{1}{2}h_1h_2^2 + \tfrac{1}{2}h_1h_3^2)u - (h_1^2h_3 + \tfrac{2}{3}h_3^3)\cos(u) - h_1h_2h_3\cos^2(u) - \tfrac{1}{3}h_2^2h_3\cos^3(u) + (h_1^2h_2 + \tfrac{2}{3}h_2^3)\sin(u) + (\tfrac{1}{2}h_1h_2^2 - \tfrac{1}{2}h_1h_3^2)\cos(u)\sin(u) + (\tfrac{1}{2}h_1h_2^2 - \tfrac{1}{2}h_1h_3^2) \times \cos(u)\sin(u) + \tfrac{1}{3}h_2^3\cos^2(u)\sin(u) - \tfrac{1}{3}h_3^3\cos(u)\sin^2(u) + \tfrac{1}{3}h_2h_3^2\sin^3(u). \tag{A1.6j}$$

Appendix 2. The range of a quadratic form over a simplex

In bandstructure calculations often the range $[\varepsilon_{\min}, \varepsilon_{\max}]$ of the (interpolated) dispersion relation $\varepsilon(\boldsymbol{k})$ has to be calculated, e.g. to narrow down the energy range in which the Fermi energy has to be searched. When using quadratic interpolation for $\varepsilon(\boldsymbol{k})$, $\varepsilon_{\min}$ and $\varepsilon_{\max}$ are also needed for accurate numerical integration of the surface integral $I(E)$ to obtain the volume integral $J(E)$ (see appendix 2 of [20]).

The range is easily calculated when using linear interpolation for $\varepsilon(\boldsymbol{k})$: $\varepsilon_{\min}$ is the minimum of $(\varepsilon_1, \varepsilon_2, \varepsilon_3, \varepsilon_4)$ and $\varepsilon_{\max}$ is the maximum of $(\varepsilon_1, \varepsilon_2, \varepsilon_3, \varepsilon_4)$, where $(\varepsilon_1, \varepsilon_2, \varepsilon_3, \varepsilon_4)$ are the energies in the four corners of the tetrahedron. When using quadratic interpolation for $\varepsilon(\boldsymbol{k})$, the calculation of the minimum and maximum energy is more involved. We construct algorithms for the one-, two- and three-dimensional case.

A2.1. The one-dimensional case

For the one-dimensional case, the simplex is an interval $[x_1, x_2]$ and the quadratic form is a parabola

$$\varepsilon(x) = q_1 + q_2 x + q_3 x^2. \tag{A2.1}$$

The parabola has two side extrema at the endpoints of the interval:

$$\varepsilon(x_1) = q_1 + q_2 x_1 + q_3 x_1^2 \tag{A2.2a}$$

$$\varepsilon(x_2) = q_1 + q_2 x_2 + q_3 x_2^2 \tag{A2.2b}$$

and has an extremum at the point x_3 where

$$\mathrm{d}\varepsilon/\mathrm{d}x = q_2 + 2q_3 x_3 = 0 \tag{A2.3}$$

with energy

$$\varepsilon(x_3) = q_1 - q_2^2/4q_3. \tag{A2.4}$$

We only have to consider extrema for which $x_1 \leqslant x_3 \leqslant x_2$. The range of the parabola is

$$[\min(\varepsilon(x_1), \varepsilon(x_2), \varepsilon(x_3)), \max(\varepsilon(x_1), \varepsilon(x_2), \varepsilon(x_3))].$$

A2.2 The two-dimensional case

For the two-dimensional case, the simplex is a triangle with corners (s_1, s_2, s_3) and the quadratic surface is an ellipse, a hyperbola, a parabola or a straight line. We first note that the range of the quadratic form

$$\varepsilon(x, y) = q_1 + q_2 x + q_3 y + q_4 x^2 + q_5 xy + q_6 y^2 \tag{A2.5}$$

is not changed by an affine transformation of both the triangle and the quadratic form. As the range is more easily calculated if the triangle is the triangle with the corners $(0, 0)$, $(0, 1)$ and $(1, 0)$, we apply the affine transformation

$$\boldsymbol{k} = s_1 + u(s_2 - s_1) + v(s_3 - s_1) \tag{A2.6}$$

where $0 \leqslant u \leqslant 1, 0 \leqslant v \leqslant 1 - u$. The quadratic form in (x, y) becomes a quadratic form in the variables (u, v)

$$\varepsilon(u, v) = q_1 + q_2 u + q_3 v + q_4 u^2 + q_5 uv + q_6 v^2. \tag{A2.7}$$

Now for each u, (A2.7) represents a parabola in the variable v. These parabolas have the 'side extrema'

$$v = 0: \qquad \varepsilon(u) = q_1 + q_2 u + q_4 u^2 \tag{A2.8a}$$

$$v = 1 - u: \qquad \varepsilon(u) = q_1 + q_3 + q_6 + (q_2 - q_3 + q_5 - 2q_6)u + (q_4 - q_5 + q_6)u^2. \tag{A2.8b}$$

So the 'side extrema' are parabolas in the variable u, and the range of the parabolas (A2.8a), which we will denote by $[\varepsilon_{\min 1}, \varepsilon_{\max 1}]$, and (A2.8$b$), which we will denote by $[\varepsilon_{\min 2}, \varepsilon_{\max 2}]$, can be calculated using the algorithm for the one-dimensional case. The parabolas (A2.7) have 'extrema' at the points $(u, v_{ext}(u))$ where

$$(\partial\varepsilon(u, v)/\partial v)|_{v=v_{ext}} = q_3 + q_5 u + 2q_6 v_{\text{ext}} = 0: \qquad v_{ext}(u) = (-q_3 - q_5 u)/2q_6 \tag{A2.9}$$

with energy

$$\varepsilon(u) = q_1 - q_3^2/4q_6 + u(q_2 - q_3 q_5/2q_6) + u^2(q_4 - q_5^2/4q_6). \tag{A2.10}$$

So the 'extrema' are also parabolas in the parameter u. We only have to consider extrema for which

$$0 \leqslant v_{ext} \leqslant 1 - u \qquad 0 \leqslant u \leqslant 1. \tag{A2.11}$$

This linear inequality can be easily solved for u and the range of the parabolas (A2.10) $[\varepsilon_{\min 3}, \varepsilon_{\max 3}]$ can be calculated using the algorithm for the one-dimensional case. Finally, the range of the quadratic form over the triangle becomes

$$[\min(\varepsilon_{\min 1}, \varepsilon_{\min 2}, \varepsilon_{\min 3}), \max(\varepsilon_{\max 1}, \varepsilon_{\max 2}, \varepsilon_{\max 3})].$$

A2.3. The three-dimensional case

For the three-dimensional case, the simplex is a tetrahedron with corners (s_1, s_2, s_3, s_4) and the quadratic form is one of the forms given in table 2. As for the two-dimensional case, we reduce the tetrahedron to the standard tetrahedron with the corners (0, 0, 0), (1, 0, 0), (0, 1, 0) and (0, 0, 1) by the affine transformation

$$k = s_1 + u(s_2 - s_1) + v(s_3 - s_1) + w(s_4 - s_1) \tag{A2.12}$$

where $0 \leqslant u \leqslant 1$, $0 \leqslant v \leqslant 1 - u$, $0 \leqslant w \leqslant 1 - u - v$. The quadratic form in (x, y, z) becomes a quadratic form in the variables (u, v, w)

$$\begin{aligned}\varepsilon(u, v, w) = {} & q_1 + q_2 u + q_3 v + q_4 w + q_5 u^2 + q_6 uv + q_7 uw + q_8 v^2 \\ & + q_9 vw + q_{10} w^2.\end{aligned} \tag{A2.13}$$

For each u and v, (A2.13) represents a parabola in the parameter w. These parabolas have 'side extrema'

$$w = 0: \qquad \varepsilon(u, v) = q_1 + q_2 u + q_3 v + q_5 u^2 + q_6 uv + q_8 v^2 \tag{A2.14a}$$

$$\begin{aligned}w = 1 - u - v: \qquad \varepsilon(u, v) = {} & q_1 + q_4 + q_{10} + u(q_2 - q_4 + q_7 - 2q_{10}) \\ & + v(q_3 - q_4 + q_9 - 2q_{10}) + u^2(q_5 - q_7 + q_{10}) \\ & + uv(q_6 - q_7 - q_9 + 2q_{10}) + v^2(q_8 - q_9 + q_{10})\end{aligned} \tag{A2.14b}$$

As can be seen from (A2.14), the 'side extrema' are two-dimensional quadratic forms in the parameters u and v, where u and v vary over the standard triangle. So the range of the 'side extrema' (A2.14a) $[\varepsilon_{\min 1}, \varepsilon_{\max 1}]$ and (A2.14b) $[\varepsilon_{\min 2}, \varepsilon_{\max 2}]$ can be calculated using the algorithm for the two-dimensional case.

The parabolas (A2.13) have 'extrema' at points $(u, v, w_{ext}(u, v))$ for which

$$(\partial\varepsilon(u, v, w)/\partial w)|_{w=w_{ext}} = q_4 + q_7 u + q_9 v + 2q_{10} w_{\text{ext}} = 0:$$

$$w_{\text{ext}} = (-q_4 - q_7 u - q_9 v)/2q_{10} \tag{A2.15}$$

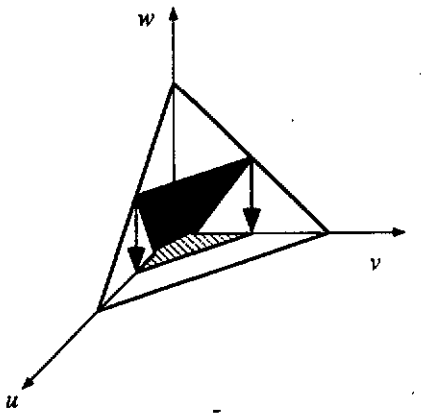

Figure A1. The solution of the inequality (A2.17) consists of the projections in (u, v) space (the lighter shaded quadrangle) of the intersection of the plane (A2.15) (the darker shaded quadrangle) with the standard tetrahedron.

with energy

$$\varepsilon(u,v) = q_1 - \frac{q_4^2}{4q_{10}} + u\left(q_2 - \frac{q_4 q_7}{2q_{10}}\right) + v\left(q_3 - \frac{q_4 q_9}{2q_{10}}\right) + u^2\left(q_5 - \frac{q_7^2}{4q_{10}}\right) + uv\left(q_6 - \frac{q_7 q_9}{2q_{10}}\right) + v^2\left(q_8 - \frac{q_9^2}{4q_{10}}\right). \tag{A2.16}$$

We only have to consider extrema for which

$$0 \leqslant w_{\text{ext}} \leqslant 1 - u - v. \tag{A2.17}$$

The solution of this inequality consists of a triangle or a quadrangle (two triangles) in the (u, v)-plane. This may be seen as follows: equation (A2.15) shows that the points $(u, v, w_{\text{ext}}(u, v))$ constitute a plane. Since only extrema inside the standard tetrahedron have to be considered, the relevant (u, v) points in the (u, v)-plane are found by the projection of the part of the $(u, v, w_{\text{ext}}(u, v))$-plane that is interior to the standard tetrahedron on the (u, v)-plane (figure A1).

As for the 'side extrema', the 'extrema' are two-dimensional quadratic forms in the parameters u and v, where u and v vary over the triangle or quadrangle, and the range of the quadratic form (A2.14) $[\varepsilon_{\text{min3}}, \varepsilon_{\text{max3}}]$ can be calculated using the algorithm for the two-dimensional case. Finally, the range of energy of the quadratic form over the tetrahedron becomes $[\min(\varepsilon_{\text{min1}}, \varepsilon_{\text{min2}}, \varepsilon_{\text{min3}}), \max(\varepsilon_{\text{max1}}, \varepsilon_{\text{max2}}, \varepsilon_{\text{max3}})]$.

References

[1] Ashcroft N W and Mermin N D 1976 *Solid State Physics* (New York: Holt-Saunders)
[2] Van Hove L 1953 *Phys. Rev.* **89** 1189
[3] Phillips J C 1956 *Phys. Rev.* **104** 1263
[4] Gilat G and Raubenheimer L J 1966 *Phys. Rev.* **144** 390
[5] Jepsen O and Andersen O K 1971 *Solid State Commun.* **9** 1763
[6] Lehmann G and Taut M 1972 *Phys. Status Solidi* b **54** 469
[7] Rath J and Freeman A J 1975 *Phys. Rev.* B **11** 2109
[8] Kaprzyk S and Mijnarends P E 1986 *J. Phys. C: Solid State Phys.* **19** 1283
[9] Kurganskii S I, Dubrovskii O I and Domashevskaya E P 1985 *Phys. Status Solidi* b **129** 293
[10] Ashraff J A and Loly P D 1987 *J. Phys. C: Solid State Phys.* **20** 4823
[11] Mueller F M, Garland J W, Cohen M H and Benneman K H 1971 *Ann. Phys., NY* **67** 19
[12] Gilat G 1972 *J. Comput. Phys.* **10** 432
[13] Reser B I 1983 *Phys. Status Solidi* b **116** 31
[14] Chen A B 1977 *Phys. Rev.* B **6** 3291

[15] Cooke J F and Wood R 1972 *Phys. Rev.* B **5** 1276
[16] MacDonald A H, Vosko S H and Coleridge P T 1979 *J. Phys. C: Solid State Phys.* **12** 2991
[17] Methfessel M S, Boon M H and Mueller F M 1983 *J. Phys. C: Solid State Phys.* **16** L949
[18] Boon M H, Methfessel M S and Mueller F M 1986 *J. Phys. C: Solid State Phys.* **19** 5337
[19] Methfessel M S, Boon M H and Mueller F M 1987 *J. Phys. C: Solid State Phys.* **20** 1069
[20] Wiesenekker G, Te Velde G and Baerends E J 1988 *J. Phys. C: Solid State Phys.* **21** 4263
[21] Jelitto J R 1969 *J. Phys. Chem. Solids* **30** 609
[22] Samuel P 1988 *Projective Geometry* (New York: Springer)
[23] Te Velde G and Baerends E J 1991 *Phys. Rev.* B (submitted)
Te Velde G 1990 *PhD Thesis* Free University, Amsterdam